Computer Systems Science & Engineering
DOI: 10.32604/csse.2023.025420
Article

Trend Autoregressive Model Exact Run Length Evaluation on a Two-Sided Extended EWMA Chart

Kotchaporn Karoon, Yupaporn Areepong* and Saowanit Sukparungsee

Department of Applied Statistics, King Mongkut's University of Technology, North Bangkok, Bangkok, 10800, Thailand
*Corresponding Author: Yupaporn Areepong. Email: yupaporn.a@sci.kmutnb.ac.th
Received: 23 November 2021; Accepted: 09 February 2022

Abstract: The Extended Exponentially Weighted Moving Average (extended EWMA) control chart is one of the control charts and can be used to quickly detect a small shift. The performance of control charts can be evaluated with the average run length (*ARL*). Due to the deriving explicit formulas for the *ARL* on a two-sided extended EWMA control chart for trend autoregressive or trend AR(p) model has not been reported previously. The aim of this study is to derive the explicit formulas for the *ARL* on a two-sided extended EWMA control chart for the trend AR(p) model as well as the trend AR(1) and trend AR(2) models with exponential white noise. The analytical solution accuracy was obtained with the extended EWMA control chart and was compared to the numerical integral equation (NIE) method. The results show that the *ARL* obtained by the explicit formula and the NIE method is hardly different, but the explicit formula can help decrease the computational (CPU) time. Furthermore, this is also expanded to comparative performance with the Exponentially Weighted Moving Average (EWMA) control chart. The performance of the extended EWMA control chart is better than the EWMA control chart for all situations, both the trend AR (1) and trend AR(2) models. Finally, the analytical solution of *ARL* is applied to real-world data in the health field, such as COVID-19 data in the United Kingdom and Sweden, to demonstrate the efficacy of the proposed method.

Keywords: Average run length; explicit formula; extended EWMA chart; trend autoregressive model

1 Introduction

The Control chart is one of the statistical process control instruments and has been applied in many fields such as finance, economics, industry, health, and medicine (see [1–5]). The concept of the control chart was initially introduced in 1931 by Shewhart [6]. The Shewhart control chart is more efficient in detecting large shifts in the processes. Next, the cumulative sum (CUSUM) [7] and the exponentially weighted moving average (EWMA) [8] control charts show that both are effective in detecting small shifts. After that, the EWMA control chart has been improved by many researchers, such as the modified exponentially weighted moving average (Modified EWMA) control chart that was originally presented by Patel et al. [9] and developed by Khan et al. [10]. These are effective in detecting small shifts quickly for observations with both autocorrelation and independently normal distribution. The extended exponentially weighted moving average (extended EWMA) control chart was proposed by Neveed et al. [11], and it is a good performance control chart for detecting small shifts in the monitored process.

The average run length (*ARL*) [12] can be used to evaluate the efficiency of control charts. It is divided into two states. For example, ARL_0 is the expected number of observations before an in-control process is taken to signal to be out of control and should be large, whereas ARL_1 is the expected number of observations taken from out of control and should be as small as possible. Previous research has shown that the *ARL* can be computed using various techniques. For instance, Areepong et al. [13] proposed the *ARL* by using the Martingale approach on the EWMA chart for exponential distribution. Chananet et al. [14] developed the *ARL* of the EWMA and CUSUM charts with a Markov chain approach based on the zero-inflated negative binomial (ZINB) model. Zhang et al. [15] proposed the *ARL* of a multivariate EWMA chart with Monte Carlo simulation. Karoon et al. [16] developed the numerical integral equation (NIE) method for evaluating the *ARL* on the extended EWMA chart for the AR(p) process.

There is a body of literature on evaluating the *ARL* with explicit formulas. Suriyakat et al. [17] derived the explicit formula for the *ARL* on the trend exponential AR(1) process in the EWMA chart. Phanyaem et al. [18] derived the *ARL* for the ARMA process via the explicit formula and the NIE method of the EWMA chart. Petcharat [19] analyzed the *ARL* by using the explicit formula on the EWMA chart for a seasonal moving average model of order q with exponential white noise. Sukparungsee et al. [20] solved the explicit formula of the *ARL* for the AR(p) model on the EWMA chart. Sunthornwat et al. [21] found the explicit formula and the optimal parameters to evaluate the *ARL* for a long-memory ARFIMA process on the EWMA chart. Recently, Supharakonsakun et al. [22] presented the exact solution of the *ARL* on the modified EWMA chart for the MA(1) process. Saghir et al. [23] proposed a modified EWMA chart that deduce the existing chart from its special cases. Aslam et al. [24] improved the Bayesian Modified EWMA location chart and its applications in the mechanical and sport industry. Phanthuna et al. [25] derived the explicit formula for the *ARL* on a modified EWMA chart for the trend stationary AR(1) model and a two-sided modified EWMA chart under the observations of AR(1) process [26]. Besides, the outbreak of COVID-19 has become a major problem facing humans all around the world. There are many literatures about control chart with the application to COVID-19 situation, such as Areepong et al. [27] derived by using quantile functions to monitor COVID-19 outbreaks via the EWMA chart based on the first hitting time of the total number of COVID-19 cases. Inkelas et al. [28] developed control charts at the country and city/neighborhood level within one state (California) to illustrate their potential value for decision-makers. However, the derivation of the explicit formula for the *ARL* on a two-sided Extended EWMA control chart for the trend AR(p) model has not been reported previously. Hence, the aim of this study is to derive the explicit formula of the *ARL* on a two-sided Extended EWMA control chart for the trend AR(p) model as well as the trend AR(1) and trend AR(2) models. The explicit formula for the *ARL* was compared with the NIE method for benchmarking. Furthermore, the explicit formulas capability for deriving the *ARL* on a two-sided Extended EWMA control chart was compared with the EWMA control chart for both simulated data and real-world data in the health field about COVID-19 data and compared.

2 Materials and Methods

2.1 Exponentially Weighted Moving Average (EWMA) Control Chart

The EWMA control chart was initially proposed by Roberts [8]. It is usually used to monitor and detect small shifts in the process. The EWMA statistic can be expressed as follows:

$$Z_t = (1-\lambda)Z_{t-1} + \lambda X_t, \ t = 1, \ 2, \ \ldots \tag{1}$$

where X_t is a process with mean, λ is an exponential smoothing parameter with $\lambda \in (0, 1]$ and Z_0 is the initial value of the EWMA statistic, $Z_0 = u$. The upper control limit (UCL) and the lower control limit (LCL) are

$$UCL = \mu + L\sigma\sqrt{\frac{\lambda}{2-\lambda}} \text{ and } LCL = \mu - L\sigma\sqrt{\frac{\lambda}{2-\lambda}} \tag{2}$$

where L is a suitable control limit width, μ is a process mean and σ is a process standard deviation.

The stopping time is given by

$$\tau_{a,h} = \inf\{t \geq 0 : Z_t < a,\ Z_t > h\} \tag{3}$$

where h is UCL and a is LCL.

2.2 Extended Exponentially Weighted Moving Average (Extended EWMA) Control Chart

The extended EWMA control chart was proposed by Neveed et al. [11]. It is developed from the EWMA control chart. That is a good performance control chart for detecting small shifts in the monitored process. The extended EWMA statistic can be expressed as follows:

$$E_t = \lambda_1 X_t - \lambda_2 X_{t-1} + (1 - \lambda_1 + \lambda_2)E_{t-1}, \quad t = 1,\ 2,\ \ldots \tag{4}$$

where X_t is a process with mean, λ_1 and λ_2 are exponential smoothing parameters with $\lambda_1 \in (0, 1)$ and $\lambda_2 \in (0, \lambda_1)$, E_0 is the initial value of the extended EWMA statistic, $E_0 = u$. The upper and lower control limits (UCL and LCL) are

$$UCL = \mu_0 + Q\sigma\sqrt{\frac{\lambda_1^2 + \lambda_2^2 - 2\lambda_1\lambda_2(1 - \lambda_1 + \lambda_2)}{2(\lambda_1 - \lambda_2) - (\lambda_1 - \lambda_2)^2}} \text{ and } LCL = \mu_0 - Q\sigma\sqrt{\frac{\lambda_1^2 + \lambda_2^2 - 2\lambda_1\lambda_2(1 - \lambda_1 + \lambda_2)}{2(\lambda_1 - \lambda_2) - (\lambda_1 - \lambda_2)^2}} \tag{5}$$

where Q is a suitable control limit width, μ is a process mean and σ is a process standard deviation.

The stopping time is given by

$$\tau_{a,b} = \inf\{t \geq 0 : E_t < a,\ E_t > b\} \tag{6}$$

where b is UCL and a is LCL.

3 Analytical Solution of ARL on a Two-Sided Extended EWMA Chart for the Trend AR(p) Model

The observations equation for the autoregressive with trend or the trend AR(p) model in the case of exponential while noise is defined as

$$X_t = \eta + \gamma t + \phi_1 X_{t-1} + \phi_2 X_{t-2} + \cdots + \phi_p X_{t-p} + \varepsilon_t \text{ or } X_t = \eta + \gamma t + \sum_{i=1}^{p} \phi_i X_{t-i} + \varepsilon_t \tag{7}$$

where η is a suitable constant, γ is a slop, ϕ_i is an autoregressive coefficient at $i = 1, 2, \ldots, p$ such that $|\phi_p| < 1$ and ε_t is white noise sequence of exponential ($\varepsilon_t \sim Exp(\alpha)$). The probability density function of ε_t is given by $f(x) = \frac{1}{\alpha}e^{-\frac{x}{\alpha}}$ where $x \geq 0$. The extended EWMA statistics E_t can be written as

$$E_t = \lambda_1\left(\eta + \gamma t + \sum_{i=1}^{p} \phi_i X_{t-i} + \varepsilon_t\right) - \lambda_2 X_{t-1} + (1 - \lambda_1 + \lambda_2)E_{t-1}$$

$$E_t = \lambda_1\eta + \lambda_1\gamma t + \lambda_1\sum_{i=1}^{p}\phi_i X_{t-i} + \lambda_1\varepsilon_t - \lambda_2 X_{t-1} + (1-\lambda_1+\lambda_2)E_{t-1}$$

$$E_t = \lambda_1\eta + \lambda_1\gamma t + (1-\lambda_1+\lambda_2)E_{t-1} + (\lambda_1\phi_1 - \lambda_2)X_{t-1} + \lambda_1\sum_{i=2}^{p}\phi_i X_{t-i} + \lambda_1\varepsilon_t. \quad (8)$$

If a and b are the lower and upper control limits of E_t for in-control process, then $a < E_t < b$.

Consequently, the extended EWMA statistics E_t can be written as

$$a \le E_t \le b$$

$$a < \lambda_1\eta + \lambda_1\gamma t + (1-\lambda_1+\lambda_2)u + (\lambda_1\phi_1 - \lambda_2)X_{t-1} + \lambda_1\sum_{i=2}^{p}\phi_i X_{t-i} + \lambda_1\varepsilon_t < b$$

$$a - \lambda_1\eta - \lambda_1\gamma t - (1-\lambda_1+\lambda_2)u - (\lambda_1\phi_1 - \lambda_2)X_{t-1} - \lambda_1$$
$$\sum_{i=2}^{p}\phi_i X_{t-i} < \lambda_1\varepsilon_t < b - \lambda_1\eta - \lambda_1\gamma t - (1-\lambda_1+\lambda_2)u - (\lambda_1\phi_1 - \lambda_2)X_{t-1} - \lambda_1\sum_{i=2}^{p}\phi_i X_{t-i}$$

$$\frac{a - \lambda_1\eta - \lambda_1\gamma t - (1-\lambda_1+\lambda_2)u - (\lambda_1\phi_1 - \lambda_2)X_{t-1} - \lambda_1\sum_{i=2}^{p}\phi_i X_{t-i}}{\lambda_1} < \varepsilon_t <$$
$$\frac{b - \lambda_1\eta - \lambda_1\gamma t - (1-\lambda_1+\lambda_2)u - (\lambda_1\phi_1 - \lambda_2)X_{t-1} - \lambda_1\sum_{i=2}^{p}\phi_i X_{t-i}}{\lambda_1}$$

$$\frac{a - (1-\lambda_1+\lambda_2)u - (\lambda_1\phi_1 - \lambda_2)X_{t-1}}{\lambda_1} - \sum_{i=2}^{p}\phi_i X_{t-i} - \eta - \gamma t < \varepsilon_t <$$
$$\frac{b - (1-\lambda_1+\lambda_2)u - (\lambda_1\phi_1 - \lambda_2)X_{t-1}}{\lambda_1} - \sum_{i=2}^{p}\phi_i X_{t-i} - \eta - \gamma t.$$

Let $L_E(u)$ denote the *ARL* on a two-sided extended EWMA control chart for the trend AR(p) model. The function $L_E(u)$ can be derived by Fredholm integral equation of the second kind [29], $L_E(u)$ is defined as follows:

$$L_E(u) = 1 + \int L(E_1)f(\varepsilon_1)d\varepsilon_1 \quad (9)$$

So, the function $L_E(u)$ is obtained as follows:

$$L_E(u) = 1 + \int_{\frac{a-(1-\lambda_1+\lambda_2)u-(\lambda_1\phi_1-\lambda_2)X_{t-1}}{\lambda_1} - \sum_{i=2}^{p}\phi_i X_{t-i} - \eta - \gamma t}^{\frac{b-(1-\lambda_1+\lambda_2)u-(\lambda_1\phi_1-\lambda_2)X_{t-1}}{\lambda_1} - \sum_{i=2}^{p}\phi_i X_{t-i} - \eta - \gamma t} L\begin{pmatrix}\lambda_1\eta + \lambda_1\gamma t + (1-\lambda_1+\lambda_2)u \\ +(\lambda_1\phi_1 - \lambda_2)X_{t-1} + \lambda_1\sum_{i=2}^{p}\phi_i X_{t-i} \\ +\lambda_1 y\end{pmatrix} f(y)dy. \quad (10)$$

Next step, Eq. (10) is changed by the variable of integration, and then $L_E(u)$ is obtained as:

$$L_E(u) = 1 + \frac{1}{\lambda_1}\int_a^b L(k) f\left(\frac{k-(1-\lambda_1+\lambda_2)u-(\lambda_1\phi_1-\lambda_2)X_{t-1}}{\lambda_1} - \sum_{i=2}^{p}\phi_i X_{t-i} - \eta - \gamma t\right) dk. \tag{11}$$

If $\varepsilon_t \sim Exp(\alpha)$, then

$$L_E(u) = 1 + \frac{e^{\frac{(1-\lambda_1+\lambda_2)u+(\lambda_1\phi_1-\lambda_2)X_{t-1}}{\lambda_1\alpha}+\frac{\sum_{i=2}^{p}\phi_i X_{t-i}+\eta+\gamma t}{\alpha}}}{\lambda_1\alpha}\int_a^b L(k)e^{-\frac{k}{\lambda_1\alpha}}dk. \tag{12}$$

when $H(u) = e^{\frac{(1-\lambda_1+\lambda_2)u+(\lambda_1\phi_1-\lambda_2)X_{t-1}}{\lambda_1\alpha}+\frac{\sum_{i=2}^{p}\phi_i X_{t-i}+\eta+\gamma t}{\alpha}}$, $K = \int_a^b L(k)e^{-\frac{k}{\lambda_1\alpha}}dk.$

Consequently,

$$L_E(u) = 1 + \frac{H(u)}{\lambda_1\alpha}K. \tag{13}$$

Consider the constant K and take turn $L(k)$ with Eq. (13),

$$K = \frac{-\lambda_1\alpha\left(e^{-\frac{b}{\lambda_1\alpha}} - e^{-\frac{a}{\lambda_1\alpha}}\right)}{1 + \frac{1}{\lambda_1-\lambda_2}\cdot e^{\frac{(\lambda_1\phi_1-\lambda_2)X_{t-1}}{\lambda_1\alpha}+\frac{\sum_{i=2}^{p}\phi_i X_{t-i}+\eta+\gamma t}{\alpha}}\cdot\left(e^{-\frac{(\lambda_1-\lambda_2)b}{\lambda_1\alpha}} - e^{-\frac{(\lambda_1-\lambda_2)a}{\lambda_1\alpha}}\right)}. \tag{14}$$

Substituting constant K form Eq. (14) into Eq. (13), then $L_E(u)$ can be written as

$$L_E(u) = 1 - \frac{(\lambda_1-\lambda_2)e^{\frac{(1-\lambda_1+\lambda_2)u}{\lambda_1\alpha}}\cdot\left(e^{-\frac{b}{\lambda_1\alpha}} - e^{-\frac{a}{\lambda_1\alpha}}\right)}{(\lambda_1-\lambda_2)e^{-\left\{\frac{(\lambda_1\phi_1-\lambda_2)X_{t-1}}{\lambda_1\alpha}+\frac{\sum_{i=2}^{p}\phi_i X_{t-i}+\eta+\gamma t}{\alpha}\right\}} + \left(e^{-\frac{(\lambda_1-\lambda_2)b}{\lambda_1\alpha}} - e^{-\frac{(\lambda_1-\lambda_2)a}{\lambda_1\alpha}}\right)}. \tag{15}$$

Finally, the solution of Eq. (15) is the explicit formula of *ARL* on a two-sided extended EWMA control chart for the trend AR(p) model. The process is in-control with the exponential parameter $\alpha = \alpha_0$, whereas the process is out-of-control with the exponential parameter $\alpha = \alpha_1$, and then $\alpha_1 = (1+\delta)\alpha_0$ where $\alpha_1 > \alpha_0$ and δ is the shift size.

4 NIE Method of ARL on a Two-Sided Extended EWMA Chart for the Trend AR(p) Model

The NIE method is one of the techniques that is used to approximate the *ARL* on a two-sided Extended EWMA chart for the trend AR(p) model. Let $L_N(u)$ be the estimated value of the *ARL* with the m linear equation systems by using the composite midpoint quadrature rule [16].

The *ARL* approximating NIE method on a two-sided extended EWMA chart is evaluated as follows:

$$\int_a^b L(k)f(k)dk \approx \sum_{j=1}^{m} w_j f(x_j) \tag{16}$$

The system of m linear equation is showed as:

$L_{m\times 1} = 1_{m\times 1} + R_{m\times m}L_{m\times 1}$ or $(I_m - R_{m\times m})L_{m\times 1} = 1_{m\times 1}$ or $L_{m\times 1} = (I_m - R_{m\times m})^{-1}1_{m\times 1}$

$L_{m\times 1} = (I_m - R_{m\times m})^{-1}1_{m\times 1},\ L_{m\times 1} = [L_{NIE}(x_1),\ L_{NIE}(x_2),\ \ldots,\ L_{NIE}(x_m)]^T,$
$I_m = diag(1,\ 1,\ \ldots,\ 1)$ and $1_{m\times 1} = [1,\ 1,\ \ldots,\ 1]^T$.

Let $R_{m\times m}$ be a matrix, the definition of the m to m^{th} element of the matrix R is given by

$$[R_{ij}] \approx \frac{1}{\lambda_1} w_j f\left(\frac{x_j - (1-\lambda_1+\lambda_2)x_i - (\lambda_1\phi_1 - \lambda_2)X_{t-1}}{\lambda_1} - \sum_{i=2}^{p}\phi_i X_{t-i} - \eta - \gamma t\right)$$

So, the solution of numerical integral equation can be explained as

$$L_N(u) = 1 + \frac{1}{\lambda_1}\sum_{j=1}^{m} w_j L(x_j) f\left(\frac{x_j - (1-\lambda_1+\lambda_2)u - (\lambda_1\phi_1 - \lambda_2)X_{t-1}}{\lambda_1} - \sum_{i=2}^{p}\phi_i X_{t-i} - \eta - \gamma t\right) \tag{17}$$

where x_j is a set of the division point on the interval $[a,\ b]$ as $x_j = \left(j - \frac{1}{2}\right)w_j + a,\ j = 1,\ 2,\ \ldots,\ m$, w_j is a weight of the composite midpoint formula $w_j = \frac{b-a}{m}$.

5 Existence and Uniqueness of ARL

By using the Banach's Fixed-Point Theorem, the *ARL* solution demonstrates that the integral equation for explicit formulas exists only once. Let T be an operation in the class of all continuous functions.

$$T(L_E(u)) = 1 + \frac{1}{\lambda_1}\int_a^b L(k) f\left(\frac{k - (1-\lambda_1+\lambda_2)u - (\lambda_1\phi_1 - \lambda_2)X_{t-1}}{\lambda_1} - \sum_{i=2}^{p}\phi_i X_{t-i} - \eta - \gamma t\right) dk \tag{18}$$

If an operator T is a contraction, then the fixed-point equation $T(L_E(u)) = L_E(u)$ has a unique solution. To show that Eq. (18) exists and has a unique solution, theorem can be used as follows below.

Theorem 1 Banach's Fixed-point Theorem: Let X be a complete metric space and $T{:}X \to X$ be a contraction mapping with contraction constant $r \in [0,\ 1)$ such that $\|T(L_1) - T(L_2)\| \le r\|L_1 - L_2\|$, $\forall L_1,\ L_2 \in X$. Then there exists a unique $L(\cdot) \in X$ such that $T(L_E(u)) = L_E(u)$, i.e., a unique fixed-point in X.

Proof: Let T defined in Eq. (18) is a contraction mapping for $L_1, L_2 \in u[a,\ b]$, such that $\|T(L_1) - T(L_2)\| \le r\|L_1 - L_2\|$, $\forall L_1,\ L_2 \in u[a,\ b]$ with $r \in [0,\ 1)$ under the norm $\|L\|_\infty = \sup_{u\in[a,b]}|L(u)|$, so

$$\|T(L_1) - T(L_2)\|_\infty = \sup_{u\in[a,b]}\left|\frac{1}{\lambda_1\alpha} e^{\frac{(1-\lambda_1+\lambda_2)u + (\lambda_1\phi_1-\lambda_2)X_{t-1}}{\lambda_1\alpha} + \frac{\sum_{i=2}^{p}\phi_i X_{t-i}+\eta+\gamma t}{\alpha}} \int_a^b (L_1(k) - L_2(k)) e^{-\frac{b}{\lambda_1\alpha}} dk\right|$$

$$\le \sup_{u\in[a,b]}\left|\|L_1 - L_2\| \frac{1}{\lambda_1\alpha} e^{\frac{(1-\lambda_1+\lambda_2)u + (\lambda_1\phi_1-\lambda_2)X_{t-1}}{\lambda_1\alpha} + \frac{\sum_{i=2}^{p}\phi_i X_{t-i}+\eta+\gamma t}{\alpha}} \cdot (-\lambda_1\alpha)\left(e^{-\frac{b}{\lambda_1\alpha}} - e^{-\frac{a}{\lambda_1\alpha}}\right)\right|$$

$$= \|L_1 - L_2\|_\infty \sup_{u\in[a,b]}\left|e^{\frac{(1-\lambda_1+\lambda_2)u + (\lambda_1\phi_1-\lambda_2)X_{t-1}}{\lambda_1\alpha} + \frac{\sum_{i=2}^{p}\phi_i X_{t-i}+\eta+\gamma t}{\alpha}}\right|\left|e^{-\frac{a}{\lambda_1\alpha}} - e^{-\frac{b}{\lambda_1\alpha}}\right| \le r\|L_1 - L_2\|_\infty$$

6 Comparing the ARL Results

According to Eq. (17), the *ARL* of the NIE method is approximated by division points m = 1,000 nodes. The solution of the NIE method is compared to the explicit formula for the trend AR(p) model on the extended EWMA chart by using the computation time (CPU time) and the absolute percentage relative error (APRE) [30], which can be computed as

$$APRE(\%) = \frac{|L_E(u) - L_N(u)|}{L_E(u)} \times 100 \tag{19}$$

The speed test results were computed by the CPU time (PC System: windows10, 64-bit, Intel® Core™ i5-8250U 1.60, 1.80 GHz, RAM 4 GB) in seconds. In addition, the numerical results were computed by MATHEMATICA. The initial parameter value was studied at ARL_0 = 370 on a two-sided extended EWMA chart for the trend AR(p) model namely the trend AR(1) and trend AR(2) models with exponential white noise and given $\lambda_1 = 0.05$, $\lambda_2 = 0.01$. The in-control process was presented a parameter value as $\alpha = \alpha_0$ with shift size ($\delta = 0$). On the other hand, the out-of-control process was presented parameter values as $\alpha_1 = (1+\delta)\alpha_0$ with shift sizes (δ = 0.001, 0.003, 0.005, 0.010, 0.030, 0.050, 0.100, 0.500, 1.000). Moreover, the coefficient parameters of the process ($\phi_1 = 0.1, -0.1$) and ($\phi_1 = 0.1$, $\phi_2 = 0.1, -0.1$) were used for the trend AR(1) model, and the trend AR(2) model, respectively. The process has determined that slope γ equals 0.1.

The performance comparisons of the explicit formula (as Eq. (15)) and NIE method (as Eq. (17)) are explained with *ARL*. In Tabs. 1 and 2, the *ARL* values derived from the explicit formula can help decrease the CPU time. The analytical results agree with NIE approximations with an APRE(%) less than 0.0000043% and 0.0000035%, and then the CPU time of approximately 8.8–10.5 and 9.3–11.5 s, for the trend AR(1) and trend AR(2) models, respectively, whereas the CPU time of the explicit formulas is less than 0.1 s, as well as the trend AR(1) and trend AR(2) models

Table 1: Comparing *ARL* values on the extended EWMA control chart for the trend AR(1) model using explicit formulas against the NIE method given $\lambda_1 = 0.05$, $\lambda_2 = 0.01$, $\eta = 0$, $a = 0$, $\gamma = 0.1$ for ARL_0 = 370

Shift size (δ)	$\phi_1 = 0.1$			$\phi_1 = -0.1$		
	Explicit ($L(u)$) (CPU time)	NIE ($L_{NIE}(u)$) (CPU time)	APRE(%)	Explicit ($L(u)$) (CPU time)	NIE ($L_{NIE}(u)$) (CPU time)	APRE(%)
0.000	370.0028282 (<0.1)	370.0028124 (9.985)	0.0000043	370.0022007 (<0.1)	370.0021940 (8.907)	0.0000018
0.001	222.6285267 (<0.1)	222.6285189 (9.672)	0.0000035	207.5881058 (<0.1)	207.5881027 (8.828)	0.0000015
0.003	124.2572117 (<0.1)	124.2572081 (8.906)	0.0000030	110.8824977 (<0.1)	110.8824963 (8.797)	0.0000013
0.005	86.39599653 (<0.1)	86.39599417 (9.781)	0.0000027	75.85371836 (<0.1)	75.85371747 (10.468)	0.0000012
0.010	49.34352289 (<0.1)	49.34352166 (9.266)	0.0000025	42.66567897 (<0.1)	42.66567851 (9.750)	0.0000011
0.030	18.74823467 (<0.1)	18.74823426 (9.000)	0.0000022	16.04073087 (<0.1)	16.04073071 (8.953)	0.0000010

(Continued)

Table 1 (continued)

Shift size (δ)	$\phi_1 = 0.1$			$\phi_1 = -0.1$		
	Explicit ($L(u)$) (CPU time)	NIE ($L_{NIE}(u)$) (CPU time)	APRE(%)	Explicit ($L(u)$) (CPU time)	NIE ($L_{NIE}(u)$) (CPU time)	APRE(%)
0.050	11.91320517 (<0.1)	11.91320493 (8.828)	0.0000020	10.18682847 (<0.1)	10.18682838 (9.016)	0.0000009
0.100	6.606133419 (<0.1)	6.606133309 (9.125)	0.0000017	5.666575969 (<0.1)	5.666575929 (9.750)	0.0000007
0.500	2.217555232 (<0.1)	2.217555219 (9.546)	0.0000006	1.959621512 (<0.1)	1.959621508 (10.516)	0.0000002
1.000	1.640867750 (<0.1)	1.640867746 (9.874)	0.0000002	1.485839866 (<0.1)	1.485839865 (9.953)	0.0000001

Note: For $\phi_1 = 0.1$ ($b = 0.0375271$), $\phi_1 = -0.1$ ($b = 0.025024741$).

Table 2: Comparing *ARL* values on the extended EWMA control chart for the trend AR(2) model using explicit formulas against the NIE method given $\lambda_1 = 0.05$, $\lambda_2 = 0.01$, $\eta = 0$, $a = 0$, $\gamma = 0.1$ for $ARL_0 = 370$

Shift size (δ)	$\phi_1 = \phi_2 = 0.1$			$\phi_1 = 0.1$ $\phi_2 = -0.1$		
	Explicit ($L(u)$) (CPU time)	NIE ($L_{NIE}(u)$) (CPU time)	APRE(%)	Explicit ($L(u)$) (CPU time)	NIE ($L_{NIE}(u)$) (CPU time)	APRE(%)
0.000	370.0047719 (<0.1)	370.0047589 (9.532)	0.0000035	370.0047133 (<0.1)	370.0047008 (9.734)	0.0000034
0.001	218.9666453 (<0.1)	218.966639 (10.266)	0.0000029	218.1789684 (<0.1)	218.1789624 (9.312)	0.0000027
0.003	120.8909144 (<0.1)	120.8909115 (11.140)	0.0000024	120.1764142 (<0.1)	120.1764114 (9.782)	0.0000023
0.005	83.71006657 (<0.1)	83.71006468 (10.438)	0.0000023	83.14282505 (<0.1)	83.14282326 (11.126)	0.0000022
0.010	47.62257905 (<0.1)	47.62257806 (9.952)	0.0000021	47.26085617 (<0.1)	47.26085524 (10.453)	0.0000020
0.030	18.04477709 (<0.1)	18.04477677 (11.547)	0.0000018	17.89740758 (<0.1)	17.89740727 (9.735)	0.0000017
0.050	11.46428946 (<0.1)	11.46428927 (11.047)	0.0000017	11.37026579 (<0.1)	11.37026561 (10.531)	0.0000016
0.100	6.362069199 (<0.1)	6.362069111 (9.969)	0.0000014	6.310913041 (<0.1)	6.310912957 (10.564)	0.0000013
0.500	2.150983712 (<0.1)	2.150983702 (9.547)	0.0000005	2.136969812 (<0.1)	2.136969802 (9.453)	0.0000004
1.000	1.600855788 (<0.1)	1.600855785 (9.968)	0.0000002	1.592424578 (<0.1)	1.592424575 (10.297)	0.0000002

Note: For $\phi_1 = \phi_2 = 0.1$ ($b = 0.034250633$), $\phi_1 = 0.1$, $\phi_2 = -0.1$ ($b = 0.033562842$).

7 Performance Comparing the ARL Results

The relative mean index (*RMI*) [31] is used to test the performance of a two-sided extended EWMA control chart on different bound control limits $[a, b]$ and the comparative performance of the *ARL* under various λ conditions. The *RMI* can be computed as

$$RMI = \frac{1}{n}\sum_{i=1}^{n}\left[\frac{ARL_i(c) - ARL_i(s)}{ARL_i(s)}\right] \tag{20}$$

where $ARL_i(c)$ is the *ARL* of the control chart for the shift size of row i, $ARL_i(s)$ is the smallest *ARL* of all of the control chart for the shift size of row i. The control chart's *RMI* value was the lowest, indicating that the control chart had the best performance at change detection.

For Tabs. 3 and 4, the *ARL* results with $\lambda_1 = 0.05$, $\lambda_2 = 0.01$, $\gamma = 0.1$, $\eta = 0$ and $ARL_0 = 370$ show that the performance of a two-sided extended EWMA control chart under various bound control limits $[a, b]$, that were compared for, $a = 0, 0.01, 0.03, 0.05$ and $\phi_1 = 0.2, -0.2$(as the trend AR(1) model) and $\phi_1 = 0.2$, $\phi_2 = 0.2, -0.2$ (as the trend AR(2) model). The *RMI* values of the lower bound $a = 0.05$ are 0. The lower bound is higher indicated that the extended EWMA chart is more efficient for detecting shifts both two models.

Table 3: Comparing *ARL* values on the extended EWMA control chart for the trend AR(1) model with difference control bounds given $\lambda_1 = 0.05$, $\lambda_2 = 0.01$, $\eta = 0$, $\gamma = 0.1$ for $ARL_0 = 370$

ϕ_1	Shift size	$a = 0$	$a = 0.01$	$a = 0.03$	$a = 0.05$
0.2	0.000	($b = 0.04599636$) 370	($b = 0.05638784$) 370	($b = 0.07717333$) 370	($b = 0.09796482$) 370
	0.001	231.650	215.150	180.897	146.963
	0.003	132.865	117.512	89.966	67.222
	0.005	93.365	81.082	60.171	43.907
	0.010	53.871	46.024	33.302	23.919
	0.030	20.616	17.507	12.640	9.174
	0.050	13.106	11.188	8.197	6.071
	0.100	7.252	6.292	4.786	3.706
	0.500	2.391	2.231	1.965	1.756
	1.000	1.744	1.681	1.569	1.476
RMI		0.784	0.584	0.253	0
		($b = 0.02044937$)	($b = 0.03062317$)	($b = 0.05097111$)	($b = 0.0713209$)
−0.2	0.000	370	370	370	370
	0.001	200.983	183.627	149.271	117.348
	0.003	105.355	91.864	68.568	50.183
	0.005	71.594	61.491	44.788	32.225
	0.010	40.025	33.970	24.335	17.375
	0.030	14.987	12.722	9.207	6.727
	0.050	9.517	8.145	6.019	4.519
	0.100	5.302	4.633	3.588	2.841
	0.500	1.860	1.760	1.594	1.464
	1.000	1.426	1.389	1.325	1.271
RMI		0.793	0.588	0.250	0

Table 4: Comparing *ARL* values on the extended EWMA control chart for the trend AR(2) model with difference control bounds given $\lambda_1 = 0.05$, $\lambda_2 = 0.01$, $\eta = 0$, $\gamma = 0.1$, $\phi_1 = 0.2$ for ARL_0 = 370

ϕ_2	Shift size	$a = 0$	$a = 0.01$	$a = 0.03$	$a = 0.05$
0.2	0.000	($b = 0.042397$) 370	($b = 0.05275771$) 370	($b = 0.07348127$) 370	($b = 0.09421014$) 370
	0.001	227.892	211.209	176.806	142.998
	0.003	129.210	114.050	86.999	64.802
	0.005	90.386	78.367	57.992	42.221
	0.010	51.924	44.313	32.010	22.963
	0.030	19.810	16.818	12.140	8.814
	0.050	12.591	10.749	7.880	5.844
	0.100	6.974	6.054	4.613	3.580
	0.500	2.317	2.166	1.913	1.715
	1.000	1.700	1.640	1.535	1.447
RMI		0.787	0.586	0.254	0
		($b = 0.04070613$)	($b = 0.05105241$)	($b = 0.07174692$)	($b = 0.09244642$)
−0.2	0.000	370	370	370	370
	0.001	226.072	209.328	174.880	141.146
	0.003	127.489	112.431	85.623	63.687
	0.005	88.995	77.106	56.987	41.447
	0.010	51.022	43.523	31.416	22.525
	0.030	19.438	16.500	11.911	8.650
	0.050	12.353	10.548	7.735	5.739
	0.100	6.845	5.944	4.534	3.522
	0.500	2.282	2.135	1.889	1.696
	1.000	1.680	1.621	1.519	1.434
RMI		0.788	0.586	0.254	0

Besides, a two-sided extended EWMA control chart under various conditions ($\lambda_2 = 0.01, 0.02, 0.04$) are compared to the EWMA control chart ($\lambda_2 = 0$) at $\lambda_1 = 0.05, 0.10$, $\gamma = 0.1$, $\eta = 0$, $a = 0.05$ and ARL_0 = 370 for $\phi_1 = 0.3$ (as the trend AR(1) model) and $\phi_1 = \phi_2 = 0.3$ (as the trend AR(2) model). The lower and upper control limits of the EWMA and extended EWMA control charts for the trend AR(1) and trend AR(2) models are obtained in Tabs. 5 and 6. The results in Tabs. 7 and 8 show that the *RMI* value of $\lambda_1 =$ 0.05 is equal to 0. The exponential smoothing parameter of 0.05 is recommended. In addition, the *RMI* results show that the extended EWMA chart with $\lambda_2 = 0.04$(EEWMA0.04), ($RMI = 0$) had fewer *RMI* values than the extended EWMA chart with either $\lambda_2 = 0.01$(EEWMA0.01) or $\lambda_2 = 0.02$(EEWMA0.02) and the EWMA($\lambda_2 = 0$) control chart for all situations, both the trend AR(1) and the trend AR(2) models.

Table 5: Lower control limit and upper control limit of the EWMA and the extended EWMA control charts for the trend AR(1) model given $\eta = 0$, $\gamma = 0.1$, $\phi_1 = 0.3$ for $ARL_0 = 370$

λ_1	EWMA ($\lambda_2 = 0$)	Extended EWMA					
		$\lambda_2 = 0.01$		$\lambda_2 = 0.02$		$\lambda_2 = 0.04$	
	a	h	a	b	a	b	a	b
0.05	0.05	0.1406020	0.05	0.10884124	0.05	0.08858456	0.05	0.06682472
0.10	0.05	0.2401663	0.05	0.20085810	0.05	0.17053690	0.05	0.12804540

Table 6: Lower control limit and upper control limit of the EWMA and the extended EWMA control charts for the trend AR(2) model given $\eta = 0$, $\gamma = 0.1$, $\phi_1 = \phi_2 = 0.3$ for $ARL_0 = 370$

λ_1	EWMA ($\lambda_2 = 0$)	Extended EWMA						
		$\lambda_2 = 0.01$		$\lambda_2 = 0.02$		$\lambda_2 = 0.04$		
	a	h	a	b	a	b	a	b
0.05	0.05	0.1342092	0.05	0.1047736	0.05	0.08594707	0.05	0.06568533
0.10	0.05	0.2260982	0.05	0.1899824	0.05	0.16200730	0.05	0.12265030

Table 7: Comparing *ARL* values on the EWMA and the extended EWMA control charts for the trend AR(1) model given $\eta = 0$, $\gamma = 0.1$, $a = 0.05$, $\phi_1 = 0.3$ for $ARL_0 = 370$

λ_1	Shift size (δ)	EWMA ($\lambda_2 = 0$)	Extended EWMA		
			$\lambda_2 = 0.01$	$\lambda_2 = 0.02$	$\lambda_2 = 0.04$
0.05	0.000	370	370	370	370
	0.001	206.213	158.863	135.905	108.374
	0.003	109.835	74.781	60.584	45.468
	0.005	75.160	49.233	39.305	29.076
	0.010	42.422	26.969	21.320	15.653
	0.030	16.237	10.324	8.202	6.100
	0.050	10.488	6.797	5.457	4.126
	0.100	6.049	4.103	3.368	2.628
	0.500	2.375	1.881	1.649	1.400
	1.000	1.860	1.561	1.402	1.229
RMI (λ_1)		0	0	0	0
RMI (λ_2)		1.133	0.504	0.257	0
0.10	0.000	370	370	370	370
	0.001	260.799	228.889	208.561	182.362
	0.003	164.213	130.260	111.791	90.978
	0.005	120.038	91.303	76.646	60.892

(Continued)

Table 7 (continued)

λ_1	Shift size (δ)	EWMA ($\lambda_2 = 0$)	Extended EWMA		
			$\lambda_2 = 0.01$	$\lambda_2 = 0.02$	$\lambda_2 = 0.04$
	0.010	72.088	52.625	43.301	33.700
	0.030	28.412	20.265	16.515	12.749
	0.050	18.095	12.981	10.619	8.240
	0.100	9.939	7.309	6.061	4.778
	0.500	3.111	2.576	2.272	1.918
	1.000	2.196	1.919	1.743	1.523
RMI (λ_1)		0.467	0.624	0.674	0.745
RMI (λ_2)		0.791	0.405	0.21	0

Table 8: Comparing *ARL* values on the EWMA and the extended EWMA control charts for the trend AR(2) model given $\eta = 0$, $\gamma = 0.1$, $a = 0.05$, $\phi_1 = \phi_2 = 0.3$ for $ARL_0 = 370$

λ_1	Shift size (δ)	EWMA $\lambda_2 = 0$)	Extended EWMA		
			$\lambda_2 = 0.01$	$\lambda_2 = 0.02$	$\lambda_2 = 0.04$
0.05	0.000	370	370	370	370
	0.001	194.938	154.309	133.141	106.664
	0.003	100.661	71.834	58.977	44.594
	0.005	68.169	47.146	38.200	28.495
	0.010	38.149	25.769	20.700	15.336
	0.030	14.584	9.871	7.970	5.983
	0.050	9.462	6.511	5.310	4.051
	0.100	5.518	3.947	3.286	2.587
	0.500	2.255	1.833	1.621	1.386
	1.000	1.793	1.528	1.382	1.219
RMI (λ_1)		0	0	0	0
RMI (λ_2)		0.853	0.475	0.248	0
0.10	0.000	370	370	370	370
	0.001	248.774	221.608	203.526	179.223
	0.003	150.619	123.403	107.551	88.683
	0.005	108.242	85.787	73.372	59.201
	0.010	63.899	49.071	41.271	32.694
	0.030	24.929	18.824	15.710	12.359
	0.050	15.911	12.074	10.111	7.992
	0.100	8.827	6.832	5.787	4.642

(Continued)

Table 8 (continued)

λ_1	Shift size (δ)	EWMA $\lambda_2 = 0$)	Extended EWMA		
			$\lambda_2 = 0.01$	$\lambda_2 = 0.02$	$\lambda_2 = 0.04$
	0.500	2.900	2.463	2.199	1.877
	1.000	2.091	1.855	1.698	1.497
RMI (λ_1)		0.448	0.593	0.649	0.729
RMI (λ_2)		0.672	0.364	0.194	0

The results indicate that the performances of the control charts were, in ascending order, the extended EWMA with $\lambda_2 = 0.04$, extended EWMA with $\lambda_2 = 0.02$, extended EWMA with $\lambda_2 = 0.01$ and EWMA control charts, as illustrated in Figs. 1 and 2.

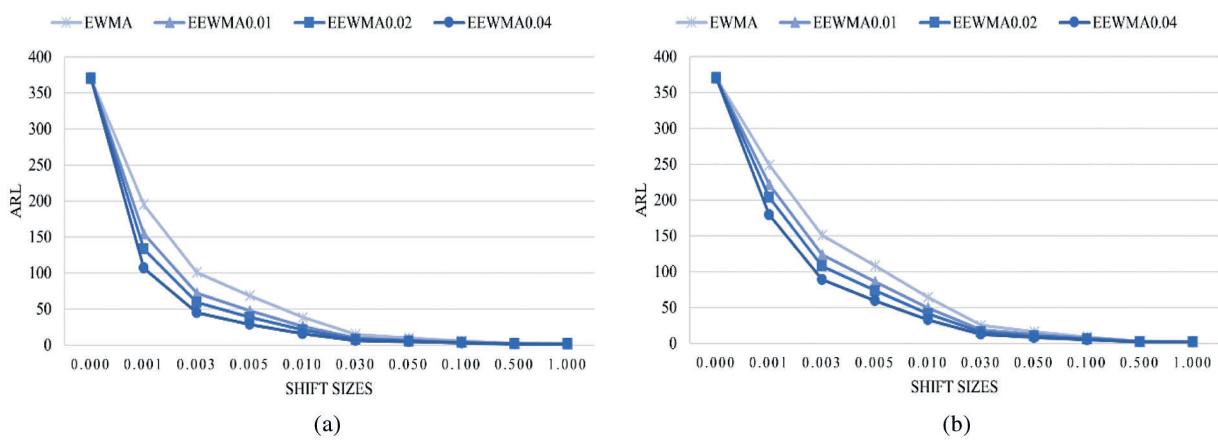

Figure 1: *ARL* values on the EWMA and the extended EWMA control charts for the trend AR(1) model with ARL_0 = 370; (a) $\lambda_1 = 0.05$ and (b) $\lambda_1 = 0.10$

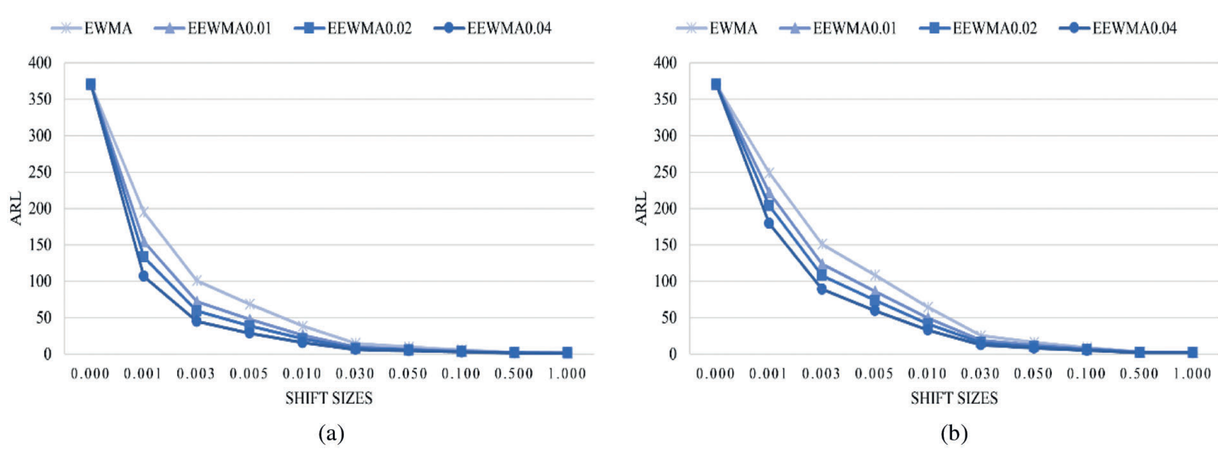

Figure 2: *ARL* values on the EWMA and the extended EWMA control charts for the trend AR(2) model with ARL_0 = 370; (a) $\lambda_1 = 0.05$ and (b) $\lambda_1 = 0.10$

8 Application to Real Data

The *ARL* was constructed using explicit formulas on a two-sided extended EWMA control chart with ARL_0 = 370 for $\lambda_1 = 0.05$ and various $\lambda_2 = 0.01$, 0.02, 0.04, and its performance was compared with the EWMA ($\lambda_2 = 0$) control chart using data on the number of COVID-19 patients in hospitals per million people in the United Kingdom and Sweden. The observations were made daily from June 26th to September 10th, 2021 and from January 24th to April 20th, 2021, respectively. This data is a stationary time series by looking at the autocorrelation function (ACF) and partial autocorrelation function (PACF). The dataset for the trend AR(1) model was assigned as the significance of the mean and standard deviation were 79.32026 and 27.69376, respectively. The trend AR(p) model in Eq. (7), the observations of the trend AR(1) model was defined as $X_t = (0.810841)t + (0.964959)X_{t-1} + \varepsilon_t$ and the error was exponential white noise ($\alpha_0 = 1.684939$). Meanwhile, the observations of the trend AR(2) model was defined as $X_t = (0.592171)t + (0.744252)X_{t-1} + (0.219693)X_{t-2} + \varepsilon_t$ and the error was exponential white noise ($\alpha_0 = 0.544925$). The *RMI* results show that the extended EWMA with $\lambda_2 = 0.04$ chart reduced the *RMI* values more than the extended EWMA chart with either $\lambda_2 = 0.01$ or $\lambda_2 = 0.02$ and the EWMA control chart for all situations, both the trend AR(1) and trend AR(2) models. The results in Tab. 9 agree with the simulation results in Tab. 7. Similarly, the results in Tab. 10 agree with the simulation results in Tab. 8.

Table 9: Comparing *ARL* values on the EWMA and the extended EWMA control chart for the trend AR(1) model with number of COVID-19 patients in hospitals per million people in United Kingdom given $\lambda_1 = 0.05$, $\eta = 0$, $a = 0.05$, $\gamma = 0.810841$, $\phi_1 = 0.964959$, $\alpha = 1.684939$ for ARL_0 = 370

Shift size (δ)	EWMA ($\lambda_2 = 0$)	Extended EWMA		
		$\lambda_2 = 0.01$	$\lambda_2 = 0.02$	$\lambda_2 = 0.04$
	($h = 0.2275289$)	($b = 0.1864128$)	($b = 0.1555061$)	($b = 0.1138792$)
0.000	370	370	370	370
0.001	269.483	223.565	198.024	168.576
0.003	174.783	125.164	103.107	81.180
0.005	129.487	87.194	70.000	53.760
0.010	78.829	49.985	39.232	29.525
0.030	31.274	19.215	14.951	11.191
0.050	19.846	12.335	9.658	7.284
0.100	10.775	6.990	5.578	4.292
0.500	3.238	2.537	2.192	1.823
1.000	2.265	1.915	1.714	1.479
RMI	1.117	0.491	0.240	0

Hence, the extended EWMA ($\lambda_2 = 0.04$) and EWMA ($\lambda_2 = 0$) control charts were plotted by calculating E_t and Z_t for the two datasets when given $\lambda_1 = 0.05$. Detecting the process with real data of the number of COVID-19 patients in hospitals per million people in the United Kingdom and Sweden were shown in Figs. 3 and 4, respectively. In Fig. 3, the *ARL* of the extended EWMA and EWMA control charts indicates that, the process was signaled as out-of-control at the 7th and 13th observations, respectively. In

Fig. 4, the *ARL* of the extended EWMA and EWMA control charts indicates that the process was signaled as out-of-control at the 1st and 27th observations, respectively. As a result, a two-sided extended EWMA control chart can detect shifts faster than the EWMA control chart.

Table 10: Comparing *ARL* values on the EWMA and the extended EWMA control chart for the trend AR(2) model with number of COVID-19 patients in hospitals per million people in Sweden given $\lambda_1 = 0.05$, $\eta = 0$, $a = 0.05$, $\gamma = 0.592171$, $\phi_1 = 0.744252$, $\phi_2 = 0.219693$, $\alpha = 0.544925$ for $ARL_0 = 370$

Shift size (δ)	EWMA ($\lambda_2 = 0$)	Extended EWMA		
		$\lambda_2 = 0.01$	$\lambda_2 = 0.02$	$\lambda_2 = 0.04$
	($h = 0.10722551$)	($b = 0.07608989$)	($b = 0.06214202$)	($b = 0.052679536$)
0.000	370	370	370	370
0.001	166.252	84.701	63.958	42.457
0.003	79.672	33.997	24.756	15.968
0.005	52.719	21.615	15.680	10.147
0.010	28.983	11.715	8.556	5.656
0.030	11.079	4.794	3.642	2.597
0.050	7.272	3.378	2.644	1.978
0.100	4.367	2.309	1.890	1.512
0.500	2.016	1.443	1.275	1.128
1.000	1.699	1.318	1.185	1.073
RMI	2.443	0.691	0.334	0

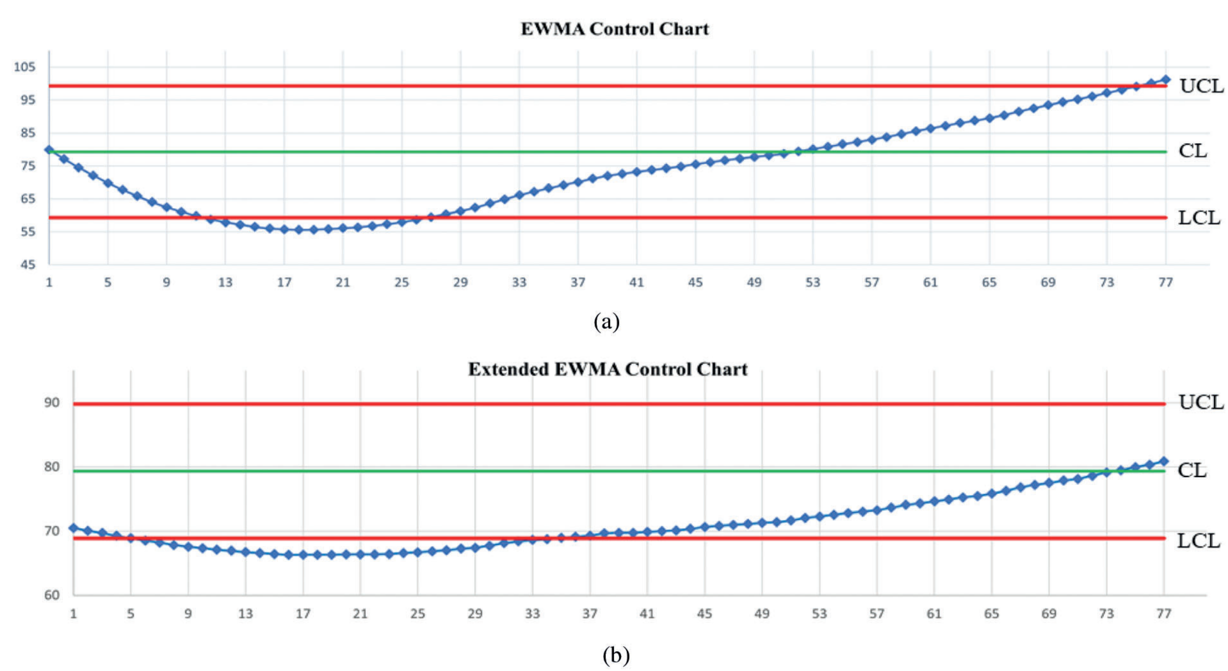

Figure 3: Detecting the number of COVID-19 patients in hospitals in the United Kingdom when given $ARL_0 = 370$ under the trend AR(1) model on (a) EWMA chart and (b) Extended EWMA chart at $\lambda_2 = 0.04$.

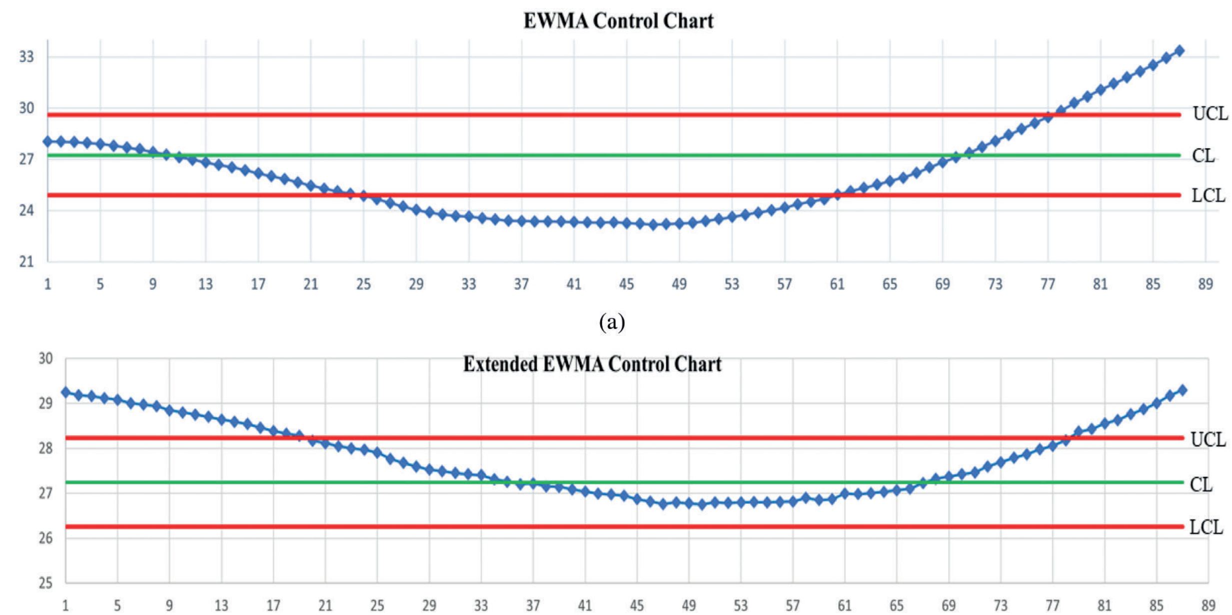

(a)
(b)

Figure 4: Detecting the number of COVID-19 patients in hospitals in Sweden when given $ARL_0 = 370$ under the trend AR(2) model on (a) EWMA chart and (b) Extended EWMA chart at $\lambda_2 = 0.04$.

9 Discussions and Conclusions

The performances of control charts were evaluated by using *ARL*. The explicit formulas comprise a good alternative to the NIE method for constructing the *ARL*, both the trend AR(1) and trend AR(2) models. The performance comparison of the *ARL* using explicit formulas on a two-sided extended EWMA on different bound control limits [a, b] and the comparative performance of the *ARL* under various λ conditions is further tested by using the relative mean index (*RMI*). The *RMI* values of the lower bound ($a = 0.05$) are 0. The extended EWMA control chart has given a higher capability for detecting shifts if the lower bound has been higher. When the comparative performance of the *ARL* under various λ_1 conditions is examined, the *RMI* value with $\lambda_1 = 0.05$ is equal to 0. So, the exponential smoothing parameter of 0.05 is recommended. Furthermore, the extended EWMA control chart has a higher efficiency if λ_2 is increased. After that, the extended EWMA control can detect shifts faster than the EWMA control chart when the datasets were verified by calculating the control charts. Finally, the simulation study and the performance illustration with real data using data on the number of COVID-19 patients in hospitals per million people in the United Kingdom and Sweden provided similar results.

Acknowledgement: We are grateful to the referees for their constructive comments and suggestions which helped to improve this research.

Funding Statement: Thailand Science Research and Innovation Fund, and King Mongkut's University of Technology North Bangkok Contract No. KMUTNB-FF-65-45.

Conflicts of Interest: The authors declare that they have no conflicts of interest to report regarding the present study.

References

[1] M. Kovarik and L. Sarga, "Implementing control charts to corporate financial management," *WSEAS Transactions on Mathematics*, vol. 13, pp. 246–255, 2014.

[2] M. Alsaid, R. M. Kamal and M. M. Rashwan, "The performance of control charts with economics-statistical design when parameters and estimated," *Review of Economics and Political Science*, vol. 6, no. 2, pp. 142–160, 2021.

[3] S. M. Anwar, M. Aslam, S. Ahmad and M. Riaz, "A modified-mxEWMA location chart for the improved process monitoring using auxiliary information and its application in wood industry," *Quality Technology and Quantitative Management*, vol. 17, no. 5, pp. 561–579, 2020.

[4] S. Ozigen, "Statistical quality control charts: New tools for studying the body mass index of populations from the young to the elderly," *The Journal of Nutrition, Health and Aging*, vol. 15, no. 5, pp. 333–334, 2011.

[5] S. H. Steiner, K. Grant, M. Coory and H. A. Kelly, "Detecting the start of an influenza outbreak using exponentially weighted moving average charts," *BMC Medical Informatics and Decision Making*, vol. 10, no. 37, pp. 1–8, 2010.

[6] W. A. Shewhart, *Economic Control of Quality of Manufactured Product*, NY, USA: Van Nostrand, 1931.

[7] E. S. Page, "Continuous inspection schemes," *Biometrika*, vol. 41, no. 1–2, pp. 100–115, 1954.

[8] W. S. Roberts, "Control chart tests based on geometric moving averages," *Technometrics*, vol. 1, no. 3, pp. 239–250, 1959.

[9] A. K. Patel and J. Divecha, "Modified exponentially weighted moving average (EWMA) control chart for an analytical process data," *Chemical Engineering and Materials Science*, vol. 2, pp. 12–20, 2011.

[10] N. Khan, M. Alsam and C. H. Jun, "Design of a control chart using a modified EWMA statistics," *Quality and Reliability Engineering International*, vol. 33, no. 5, pp. 1095–1104, 2017.

[11] M. Neveed, M. Azam, N. Khan and M. Aslam, "Design a control chart using extended EWMA statistic," *Technologies*, vol. 6, no. 4, pp. 108–122, 2018.

[12] H. Khusna, M. Mashuri, S. Suhartono, D. D. Prastyo and M. Ahsan, "Multioutput least square SVR-based multivariate EWMA control chart: The performance evaluation and application," *Cogent Engineering*, vol. 5, no. 1, pp. 1–14, 2018.

[13] Y. Areepong and A. Novikov, "Martingale approach to EWMA control chart for changes in exponential distribution," *Journal of Quality Measurement and Analysis*, vol. 4, no. 1, pp. 197–203, 2008.

[14] C. Chananet, Y. Areepong and S. Sukparungsee, "A markov chain approach for average run length of EWMA and CUSUM control chart based on ZINB model," *International Journal of Applied Mathematics and Statistics*, vol. 53, no. 1, pp. 126–137, 2015.

[15] J. Zhang, Z. Li and Z. Wang, "Control chart based on likelihood ration for monitoring linear profiles," *Computational Statistics and Data Analysis*, vol. 53, no. 4, pp. 1440–1448, 2009.

[16] K. Karoon, Y. Areepong and S. Sukparungsee, "Numerical integral equation methods of average run length on extended EWMA control chart for autoregressive process," in *Proc. of Int. Conf. on Applied and Engineering Mathematics*, London, England, pp. 51–56, 2021.

[17] W. Suriyakat, Y. Areepong, S. Sukparungsee and G. Mititelu, "Analytical method of average run length for trend exponential AR(1) processes in EWMA procedure," *IAENG International Journal of Applied Mathematics*, vol. 42, no. 4, pp. 250–253, 2012.

[18] S. Phanyaem, Y. Areepong, S. Sukparungsee and G. Mititelu, "Explicit formulas of average run length for ARMA (1, 1)," *International Journal of Applied Mathematics and Statistics*, vol. 43, no. 13, pp. 392–405, 2013.

[19] K. Petcharat, "Explicit formula of ARL for $SMA(Q)_L$ with exponential white noise on EWMA chart," *International Journal of Applied Physics and Mathematics*, vol. 6, no. 4, pp. 218–225, 2016.

[20] S. Sukparungsee and Y. Areepong, "An explicit analytical solution of the average run length of an exponentially weighted moving average control chart using an autoregressive model," *Chiang Mai Journal of Science*, vol. 44, no. 3, pp. 1172–1179, 2017.

[21] R. Sunthornwat, Y. Areepong and S. Sukparungsee, "Average run length with a practical investigation of estimating parameters of the EWMA control chart on the long memory AFRIMA process," *Thailand Statistician*, vol. 16, no. 2, pp. 190–202, 2018.

[22] Y. Supharakonsakun, Y. Areepong and S. Sukparungsee, "The exact solution of the average run length on a modified EWMA control chart for the first-order moving average process," *ScienceAsia*, vol. 46, no. 1, pp. 109–118, 2020.

[23] A. Saghir, M. Aslam, A. Faraz, L. Ahmad and C. Heuchenne, "Monitoring process variation using modified EWMA," *Quality and Reliability Engineering International*, vol. 36, pp. 328–339, 2020.

[24] M. Alsam and S. M. Anwar, "An improved bayesian modified EWMA location chart and its applications in mechanical and sport industry," *PLOS ONE*, vol. 15, pp. e0229422, 2020.

[25] P. Phanthuna, Y. Areepong and S. Sukparungsee, "Detection capability of the modified EWMA chart for the trend stationary AR(1) model," *Thailand Statistician*, vol. 19, no. 1, pp. 70–81, 2021.

[26] P. Phanthuna, Y. Areepong and S. Sukparungsee, "Exact run length evaluation on a two-sided modified exponentially weighted moving average chart for monitoring process mean," *Computer Modeling in Engineering and Sciences*, vol. 1271, no. 1, pp. 23–40, 2021.

[27] Y. Areepong and R. Sunthornwat, "EWMA control chart based on its first hitting time and coronavirus alert levels for monitoring symmetric COVID-19 cases," *Asian Pacific Journal of Tropical Medicine*, vol. 14, no. 8, pp. 364–374, 2021.

[28] M. Inkelas, C. Blair, D. Furukawa, V. G. Manuel, J. H. Malenfant *et al.,* "Using control charts to understand community variation in COVID-19," *PLOS ONE*, vol. 16, no. 4, pp. e0248500, 2021.

[29] C. W. Champ and S. E. Rigdon, "A comparison of the markov chain and the integral equation approaches for evaluating the run length distribution of quality control charts," *Communications in Statistics-Simulation and Computation*, vol. 20, no. 1, pp. 191–203, 1991.

[30] Q. T. Nguyen, K. P. Tran, P. Castagliola, G. Celano and S. Lardiane, "One-sided synthetic control charts for monitoring the multivariate coefficient of variation," *Journal of Statistical Computation and Simulation*, vol. 89, no. 1, pp. 1841–1862, 2019.

[31] A. Tang, P. Castagliola, J. Sun and X. Hu, "Optimal design of the adaptive EWMA chart for the mean based on median run length and expected median run length," *Quality Technology and Quantitative Management*, vol. 16, no. 4, pp. 439–458, 2018.